Chemical Engineering Journal 155 (2009) 750–756

Contents lists available at ScienceDirect

Chemical Engineering Journal

journal homepage: www.elsevier.com/locate/cej

Mechanisms of in-line coalescence of two-unequal bubbles in a non-Newtonian fluid

Tsao-Jen Lin*, Gen-Ming Lin

Department of Chemical Engineering, National Chung-Cheng University, Chia-Yi 621, Taiwan, ROC

ARTICLE INFO

Article history:
Received 5 January 2009
Received in revised form 9 September 2009
Accepted 14 September 2009

Keywords:
Bubble coalescence
Non-Newtonian fluid
Particle image analyzer
Visualization

ABSTRACT

The coalescing mechanism of in-line two-unequal bubbles rising in a bubble column with a non-Newtonian fluid has been experimentally studied. The non-Newtonian fluid is the 1.5 wt% polyacryamide in demineralized water and the bubble gas is air. Both qualitative flow visualization and quantitative full-field measurements using particle image analyzer have been conducted for two examples of two-unequal bubble coalescences. The instantaneous flow structure and the shear stress contour varying in different time lags are presented. As two-unequal bubbles are getting closer, the drained liquid is circulated to the back of the trailing bubble. Due to the drainage flow and the mutual interactions, the flow structure and the shear stress contour show a dramatic change from a two independent bubbles to a single bubble. Due to encounter these dynamic flow structures, the shape of the trailing bubble also has serial changes. However, the case of large trailing bubble with large momentum can affect the deformation of the small leading bubble earlier. Due to the dragging force caused by the negative pressure and the shear-thinning effect and the pushing force caused by the viscoelastic effect, the acceleration of the trailing bubble to the leading bubble is evident. It was found that the coalescence of two-unequal bubbles has higher acceleration than the coalescence of two-equal bubbles.

1. Introduction

Bubble interactions are of considerable importance in many chemical engineering, particularly in polymer processing technology, foaming dynamics, and fermentation [1–3]. Among these intrinsic dynamic behaviors of bubble interactions, bubble coalescence is known to be a key factor for determining the efficiency of mass/heat transfers and chemical reactions between two phases [4–8]. Additionally, with existing a bubble size distribution in the reactor, the coalescence between two-unequal bubble sizes is the most common occurrence in all bubble coalescences. Some studies have been conducted to understand the coalescence process involving the two-unequal bubble sizes in a non-Newtonian fluid. However, the fundamental understanding, especially in the quantitative aspect, is currently inadequate.

Previous studies regarding the coalescing behavior for two successive bubbles have mainly focused on Newtonian fluids [9–13]. Liquid phase properties, gas distributor, and surfactant play important factors on the effect of hydrodynamics of the bubble coalescence [14–16]. Grienberger [17] found that bubble collision frequency is an essential factor for determining the occurrence of the bubble coalescence. The collision frequency is essentially influenced by the hydrodynamics of the bulk flow, including the turbulent field and difference in the rise velocity due to buoyancy and the presence of liquid velocity gradient. After the bubble collision, the coalescing processes start to take over and are generally divided into three steps: (1) the acceleration and elongation of the trailing bubble; (2) the trailing bubble overtaking the leading bubble; and (3) drainage, thinning, and rupture of the thin film of liquid separating the two bubbles [18–20]. The final criterion for determining coalescence is that the contact time of the coalescing bubbles should be longer than that for draining the film to rupturing thickness [21]. Furthermore, Tsuchiya and Fan [22] and DeNevers and Wu [23] concluded that the wake effect of the leading bubble is considered to be responsible for these coalescing interactions. They discovered that at a fixed initial vertical separation distance, the smaller the trailing bubble, the longer the coalescence time. Bhaga and Weber [24] also suggested that the trailing bubble rises at a velocity equal to its terminal velocity plus the wake velocity behind the leading bubble.

From the literatures it can be noted that there is a dramatic difference in the wake induced by a rising bubble in Newtonian and in non-Newtonian fluids [4,6,25]. Hence, the phenomenon of bubble coalescence should be different for these two kinds of liquids. In general, three types of bubble wake have been identified in Newtonian fluids, namely, the laminar wake, the transitional wake and the turbulent wake [11]. For the non-Newtonian fluids, the bubble wake is very peculiar. Unlike the wake in Newtonian fluids, which

* Corresponding author. Tel.: +886 5 2720411x33405; fax: +886 5 2720411.
E-mail address: chmtjl@ccu.edu.tw (T.-J. Lin).

1385-8947/$ – see front matter © 2009 Elsevier B.V. All rights reserved.
doi:10.1016/j.cej.2009.09.019

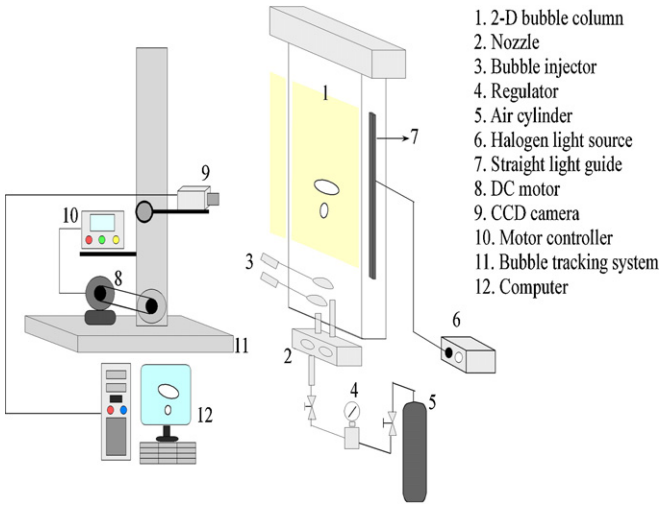

Fig. 1. Schematic diagram of the test facility.

drag the liquid along with the bubble moving upward, a negative wake in the non-Newtonian fluids is observed to push the liquid away from the bubble [26]. By laser-Doppler anemometry (LDA), Bisgaard and Hassager [27] concluded that the negative wake is induced by elasticity, which usually has an effect in the opposite direction of the inertial force. With a particle image velocimetry (PIV) technique, Funfschilling and Li [28] divided the bubble flow field into three different zones: a central down flow behind the bubble, a conical upward flow around the wake, and an upward flow zone in front of the bubble. Later, Lin and Lin [29] used a particle image analyzer (PIA) to investigate four kinds of bubble shapes (i.e., prolate-teardrop, oblate-cusped, oblate spherical-cap, and spherical-cap) in a 1.5 wt% polyacryamide non-Newtonian fluid. Through this technique and integrating calculations, they were the first to identify two pairs of axisymmetric stresses existing in the front and the rear of the bubble, which match the results of birefringence very well.

Till now, little data has been available on the bubble coalescence in non-Newtonian fluids due to the complex rheological properties resulting in a completely different flow behavior [30–36]. Most previous investigations have focused on the qualitative visualization and the quantitative measurement to examine the various intrinsic parameters (e.g., physical and rheological properties of the gas and liquid) and extrinsic parameters (e.g., the geometrical configuration of the orifice and injecting frequency) for bubbles coalescing in non-Newtonian fluids. Brindley et al. [37] showed that the half of times for squeezing films of viscoelastic liquids were two or three times higher than those of inelastic liquids. Through a high-speed cine camera, Acharya and Ulbrecht [30] reported the visualizing results of the coalescence of in-line bubbles in viscoelastic fluids. They found that due to the elasticity of non-Newtonian fluids, the

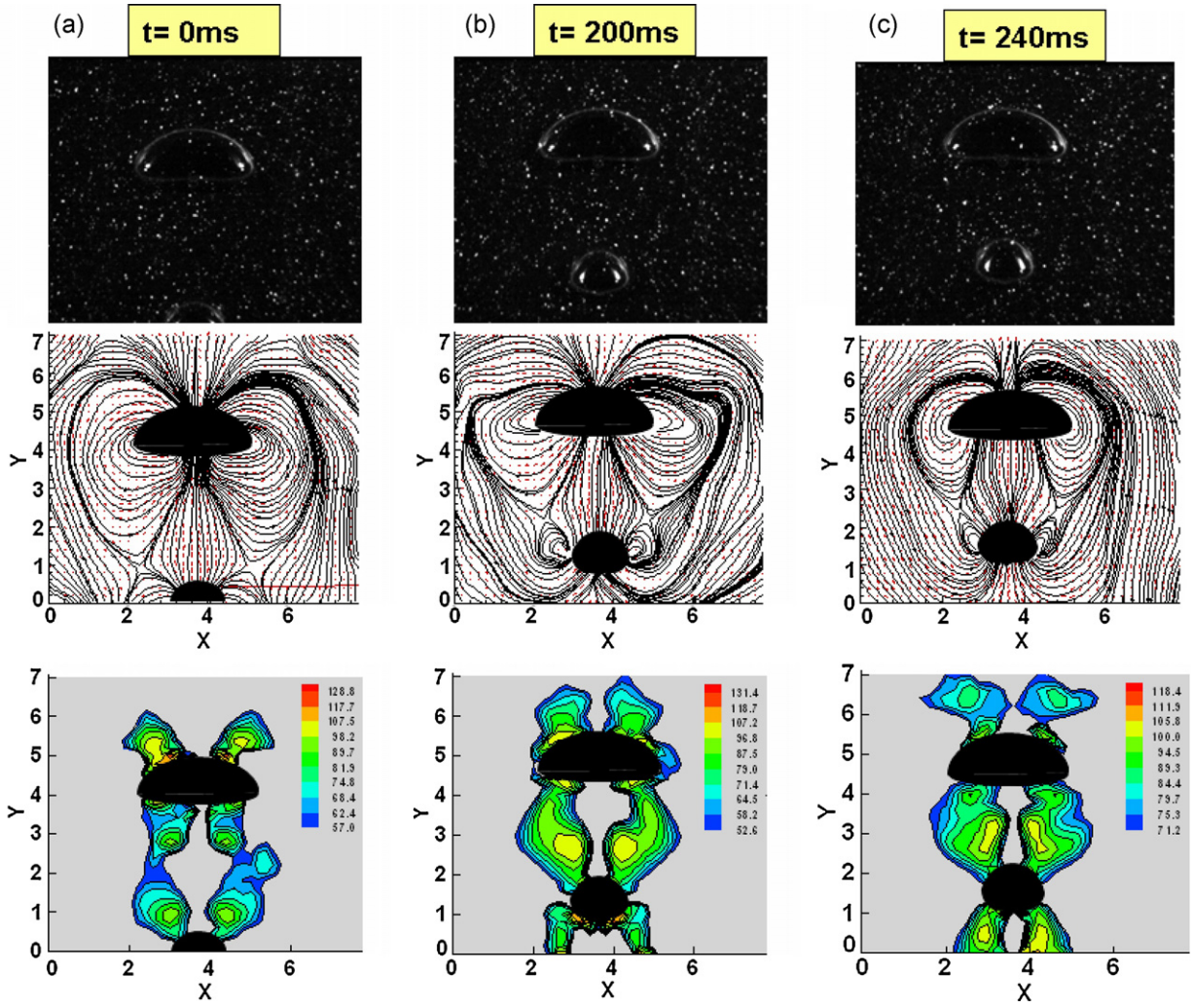

Fig. 2. (a) Original image, (b) streamline, and (c) shear stress contour for small trailing bubble coalescing with large leading bubble in a 1.5 wt% PAAm solution at different time lags.

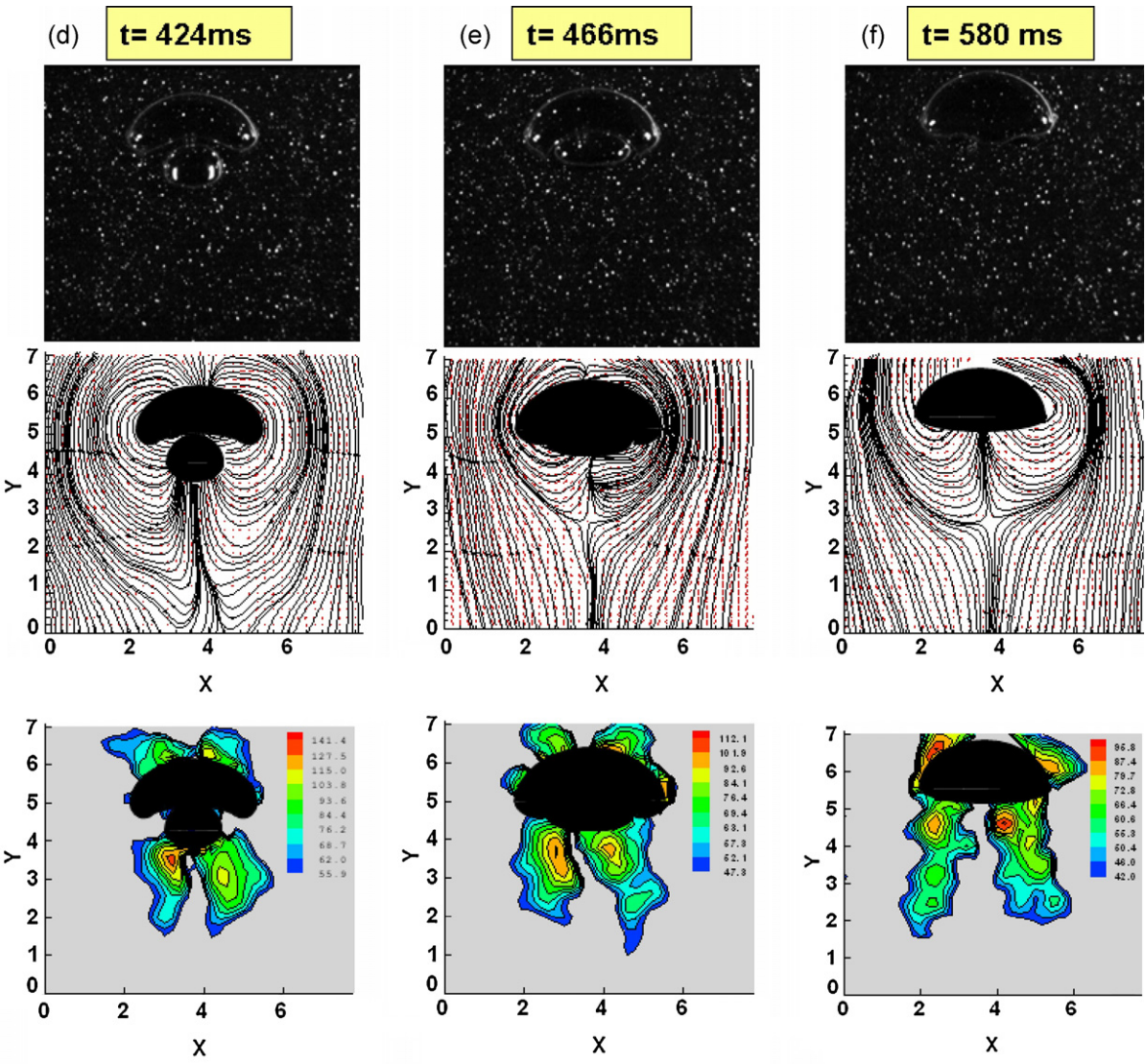

Fig. 2. (*Continued*).

wake and the drainage of the thin film are reduced, thereby increasing the collision and coalescence times of bubbles. However, no further explanation was provided in their paper.

Later, Dekee et al. [31] found that bubble coalescence in non-Newtonian fluids strongly depends on the rheological characteristics, the surfactants, and the injection frequency. Li et al. [33,34] compared the rheological simulation from a rheometer and the visualization from birefringence, concluding that the in-line interactions are primarily dominated by a mechanical competition between the creation and relaxation of stresses in fluids. They also incorporated a method of spectral analysis to investigate a threshold of injection period for the bubble interaction behaviors. But, no instantaneous information (i.e., flow field and shear stress) regarding the course of in-line bubble coalescence has been quantitatively investigated for two different size bubbles. The current study attempts to resolve this issue and provides the benchmark data for further computational modeling.

To understand the flow mechanism of in-line two-unequal bubble coalescence, it is imperative to quantify the transient flow phenomena. However, no traditional measurement techniques, neither intrusive nor non-intrusive, can provide the quantitative instantaneous flow information for an overall flow plane. Now, these measurement limitations can be overcome in the recently developed particle image analyzer (PIA). Through the utilization of advanced image acquisition and computer processing techniques, PIA can provide a quantitative means for measuring the instantaneous flow field of a plane while maintains the similar accuracy of LDA. To study the complex flow structures of the dynamic bubble coalescence, it is desirable to first examine its behavior. Furthermore, coupling the measured flow structure from PIA with the rheological data, the shear stress distribution throughout the bubble coalescence can be analyzed in this study.

2. Experimental setup

Fig. 1 shows the main features of the experimental setup, comprised of an acrylic bubble column 120 cm in height, 30 cm in width and 1.2 cm in gap thickness. Air is used as the gas phase. To avoid generating any satellite bubbles, specific volumes of air are individually pre-injected into two in-line hemispherical cup bubble injectors to generate two in-line bubbles. Two cases of bubble coalescence will be carried out: (1) small bubble to large bubble and (2) large bubble to small bubble. The non-Newtonian fluid with the rheological shear-thinning property is 1.5 wt% polyacryamide (PAAm) in demineralized water. As reported by Lin and Lin [35], the PAAm solution is a shear-thinning and viscoelastic fluid. The shear-

thinning behavior of this fluid can be described by an Ostwald-de Waele model ($\tau_{yx} = m(\gamma_{yx})^n$ with $m = 11.72$ and $n = 0.5452$). Neutrally buoyant polystyrene particles of 100 μm are used as liquid seeding particles. The concentration of seeding particles is maintained at 1% (v) to ensure that the seeding particles follow the flow closely and have virtually no effects on the flow structure. A light sheet 18 cm long generated from a straight light guide is projected from the sidewall to illuminate the tracers around the flow field. Connected with an optical fiber to the straight light guide, a 150 W halogen light source generator with a special filter lens provides a cold light to illuminate the flow field. In order to visualize the flow structure throughout all the stages of the bubble coalescence, the proper distance and injecting time lag between these two hemispherical cup bubble injectors are needed to manipulate carefully. A bubble tracking system is constructed to carry the video camera and move synchronously with the leading bubble. By adjusting the voltage of the DC motor, the synchronous movements between the tracking system and the leading bubble are accomplished. The flow field is visualized and recorded by a high-speed and high-resolution CCD camera. The shuttle speed and recording rate was 1/500 s for all the cases. Using a ruler along the flow field, the field of view is 7.8 cm × 7 cm.

A particle image analyzer (PIA) system developed by Chen and Chou [38] is applied to measure the instantaneous flow structure around two coalescing bubbles. The technique of PIA discriminates between seeding particles and bubbles based on the size of the recorded image of the objects. The vectors obtained are located at the position of the centroid of the initial tracer particle in a triplet. A commercially available program, TECPLOT, is utilized for post-processing the PIA data. For the resolution of analysis, the recorded field of view is divided into 36 × 40 grids to execute the interpolation resulting in a grid size of 2.0 mm × 2.0 mm. Execution of interpolation process using the Kriging algorithm is performed for each phase frame. For two-dimensional condition, the shear rate $\gamma_{xy}(i, j)$ of each grid point is calculated based on a finite-difference approximation for the interpolated velocity field as follows:

$$\gamma_{xy}(i,j) = \frac{\Delta u}{\Delta y} + \frac{\Delta v}{\Delta x} = \frac{u(i,j+1) - u(i,j-1)}{2\Delta y} + \frac{v(i+1,j) - v(i-1,j)}{2\Delta x} \quad (1)$$

Here $u(i, j)$ and $v(i, j)$ are the velocity components in x and y directions at the interrogation grid point (i, j), respectively; Δx and Δy are the interrogation grid intervals in x and y directions, respectively. The shear stress in each grid point can be calculated by substituting $\gamma_{xy}(i, j)$ into an Ostwald-de Waele model.

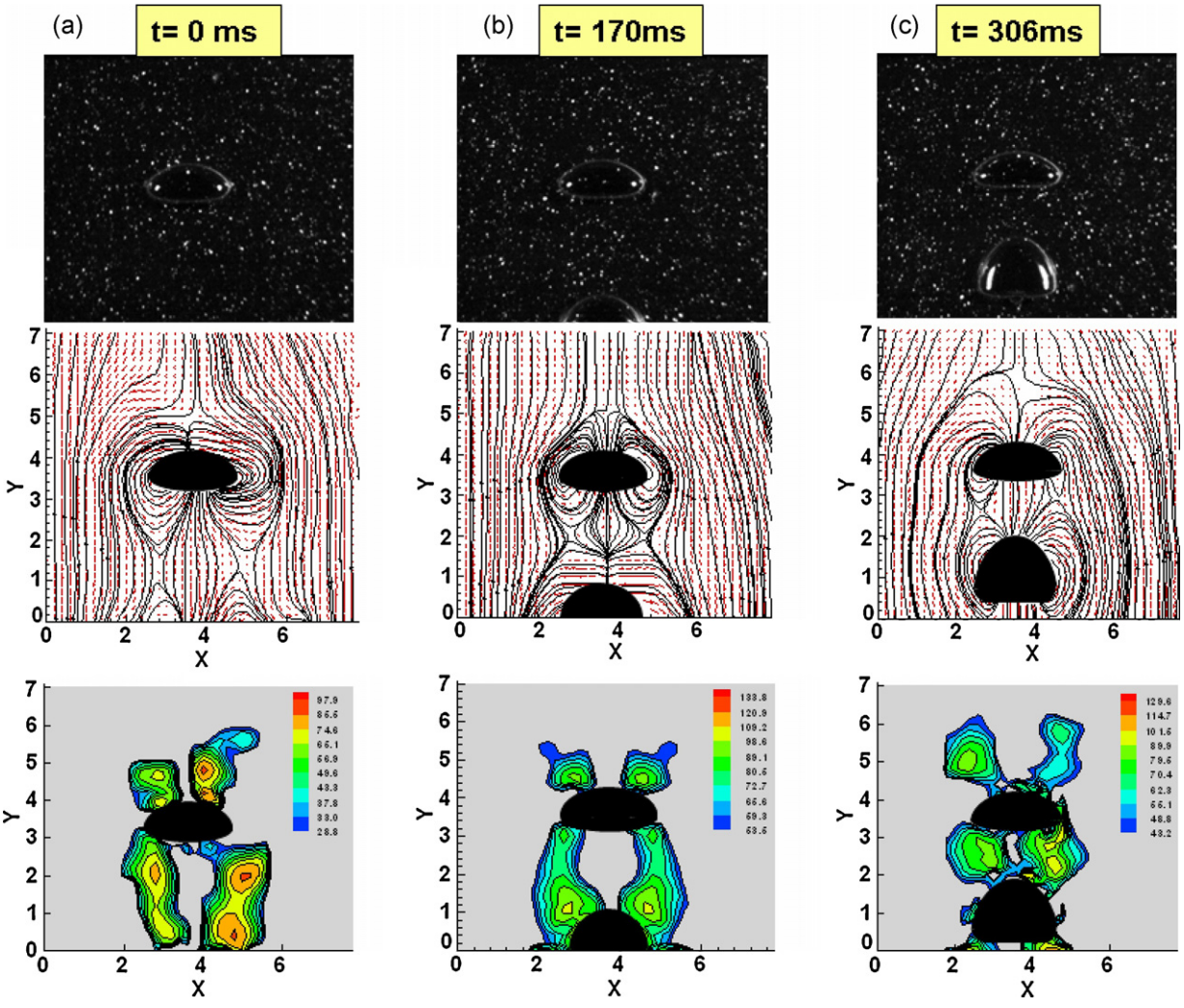

Fig. 3. (a) Original image, (b) streamline, and (c) shear stress contour for large trailing bubble coalescing with small leading bubble in a 1.5 wt% PAAm solution at different time lags.

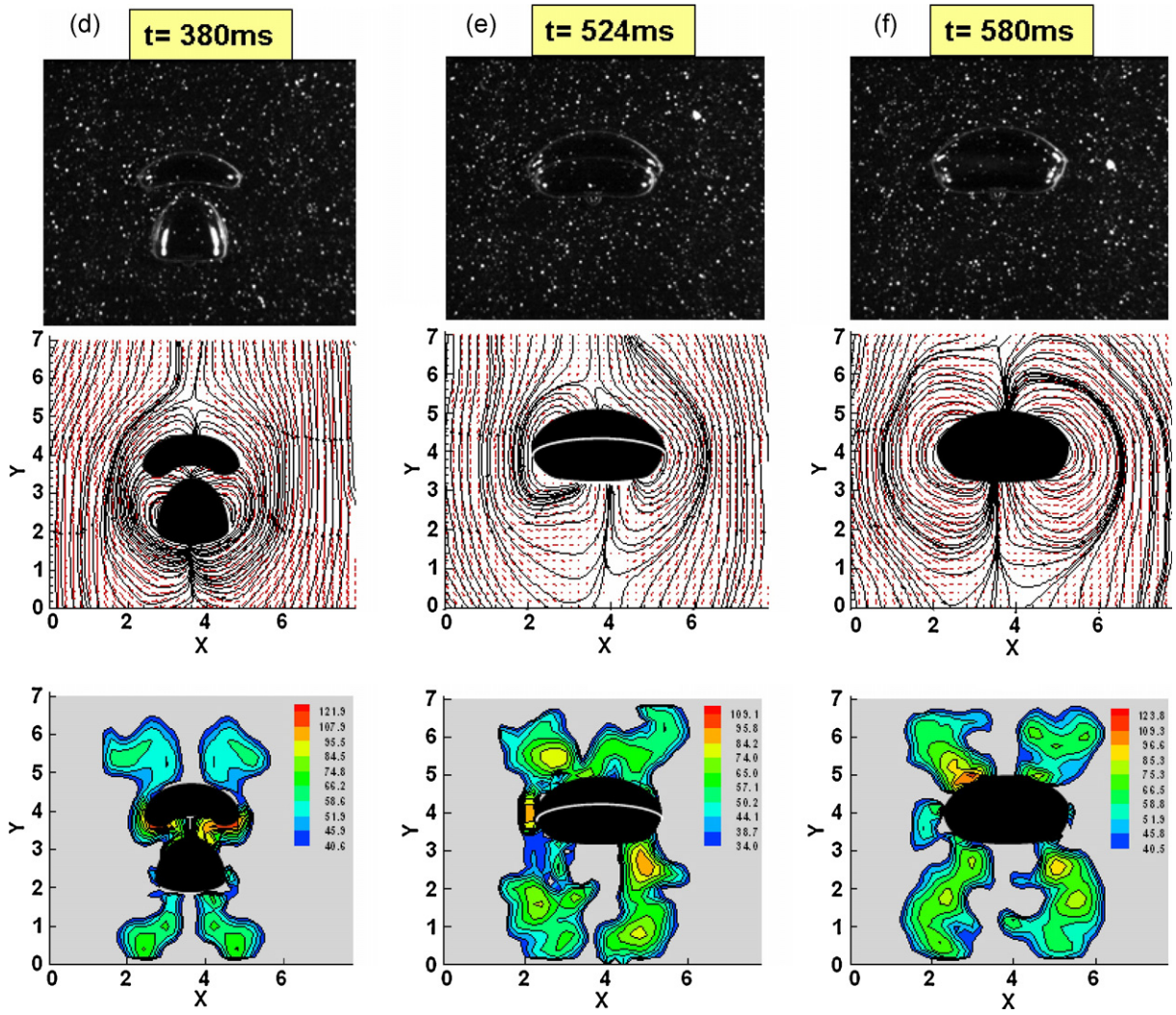

Fig. 3. (*Continued*).

3. Results and discussion

Two cases of the in-line trailing bubble coalescing with the leading bubble in a non-Newtonian fluid are presented in this study, including (i) a small trailing bubble to a large leading bubble and (ii) a large trailing bubble to a small leading bubble.

3.1. Small trailing bubble coalescing with large leading bubble

In this case, a teardrop bubble (1.45 cm in breadth and 1.1 cm in height) as a trailing bubble was introduced to coalesce with a large oblate leading bubble (2.83 cm in breadth and 1.35 cm in height). The original image, the interpolated velocity fields associated with integrated streamlines and the shear stress contour for six time lags are given in Fig. 2. To ensure the occurrence of coalescence, the small trailing bubble is introduced as close as possible to the proper place in the induced flow field of the large leading bubble. In addition, to show the time lag during the coalescing process, the first image chosen was simply denoted as the "zero" second. From the image at $t = 0$ s, it can be seen that the trailing bubble has already interacted with the leading bubble. Nevertheless, the leading bubble retained the same flow field and shear stress contour as a single oblate, as presented by Lin and Lin [29]. Due to the shear-thinning and viscoelastic effects, the liquid in front of the leading oblate bubble was compressed and circulated back to the rear of the bubble, although the negative wake disappeared and changed direction upward as it was repressed by the trailing bubble. This phenomenon of upward flow may be attributed to the lower pressure at the leading bubble wake and the shear-thinning effect causing a reduction of the apparent viscosity of the compressed liquid from the trailing bubble. Surprisingly, no shear stress was found in this upward flow region, as shown in the shear stress contour of Fig. 2(a). In addition, two pairs of axisymmetric shear stresses existed in the front and rear of the leading oblate bubble. The front pair of shear stresses of the trailing bubble started to interact with the rear pair of shear stresses of the leading bubble.

After 240 ms, the distance between the leading and trailing bubbles reached 3.2 cm. From the streamline of Fig. 2(c), the suppressed flow of the leading bubble was restrained by the trailing bubble and some part of its outer flow was circulated and sucked into the rear of the trailing bubble reducing the suppressed flow and the flattened bottom shape of the trailing bubble. Due to dragging from the top and pushing from the bottom, the trailing bubble was accelerated to come closer to the leading bubble. This acceleration further enforced the strength of the circulated flow to generate higher shear stresses in front of the trailing bubble, as shown in the shear stress contour. These higher shear stresses merged with those of the leading bubble to form a large pair of high shear stress zones. On the other hand, the upward flow did not have enough power to distort the leading bubble and became wider due to its large vol-

ume, which had a durable boundary to withstand the suppression from the upward flow.

As the time lag reached 424 ms, the trailing bubble barely contacted the leading bubble after draining out the in-between liquid. A portion of the compressed liquid from the leading bubble was circulated to the side of trailing bubble instead of flowing to the rear of the trailing bubble, as shown in Fig. 2(d). Without its own circulating flow, the trailing bubble was suppressed by the circulating flow from the leading bubble. Because this horizontal force was weaker than the vertical force generated by the circulated flow, the trailing bubble had less resistance in the *x*-direction, which led to an oblate shape without the cusp. With the suppression of the trailing bubble, the leading bubble developed a larger curvature of concavity. In general, the distribution of the shear stresses at this stage was more or less like that of a single bubble, which has two pairs of axisymmetric shear stresses with a conical shape of negative wake.

Increasing the time lag to 466 ms, the liquid thickness between the leading and trailing bubbles drained to a very thin liquid film, which is the so called "film thinning". Fig. 2(e) shows that the trailing bubble changed shape to a prolonged and flatted oblate shape, because the vertical force is stronger than the horizontal force. As it was jammed by the trailing bubble, the leading bubble was stretched to a wider and thinner shape, causing a shear stress at the latitudinal edge of the leading bubble. Finally, the liquid film was thinned down to a rupturing thickness, and then the two bubbles merged and immediately reached the stable oblate shape, as shown in Fig. 2(f).

3.2. Large trailing bubble coalescing with small leading bubble

The next experiment involved a large oblate bubble (2.20 cm in breadth and 1.54 cm in height) as a trailing bubble coalescing with a small oblate-cusped bubble (1.40 cm in breadth and 0.96 cm in height) as a leading bubble. Fig. 3 shows the original image, with the interpolated velocity fields associated with integrated streamlines and the shear stress contour at six different time lags. At the denoted zero time lag, the leading bubble has been deformed to a flat oblate bubble due to suppressed by the trailing bubble. Then the shape of leading bubble becomes progressively concave, as in the above case. On the other hand, until the time lag 380 ms, it was observed that the shape of the trailing bubble was changed to a bell shape, although its volume (or momentum) was larger than that of the leading bubble. At this time lag, the streamline in Fig. 3(d) shows that the liquid in front of the leading bubble is no longer circulating back behind itself but to the rear of trailing bubble. The liquid in front of the trailing bubble was suppressed and sucked back the rear of the trailing bubble due to the viscoelastic effect. The liquid drainage causes a high shear stress at the rear edge of the leading bubble, as shown in Fig. 3(d).

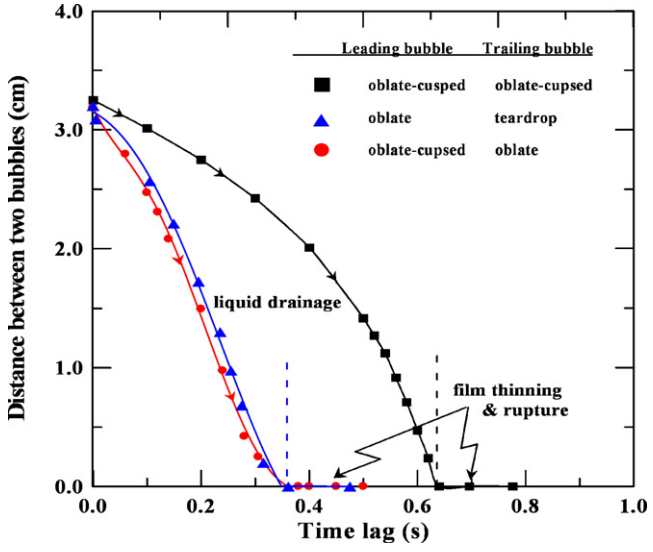

Fig. 4. Distance between two bubbles coalescing in a 1.5 wt% PAAm solution at different time lags.

The film thinning started to take over after drainage. Since there was no other space except the liquid film between two coalescing bubbles, the leading bubble was further stretched to a thinner concave shape to cover the trailing bubble. Meanwhile, the trailing bubble also changed from a bell shape to a convex shape through the circulated flow compression and the leading bubble retardation. Generally speaking, the distribution of the shear stresses at this stage is more or less like that of a single bubble, with two pairs of axisymmetric shear stresses, as shown in Fig. 3(e). It should be noted that the whole bubble is still unstable due to the unbalanced forces on its surface. With a tiny disturbance, the liquid film ruptured, and then a stable oblate shape was formed, as shown in Fig. 3(f).

3.3. Comparison of coalescing time lags

Fig. 4 shows the time lag in each stage versus the distance between two bubbles for three different cases of bubble coalescence, i.e., an two-equal oblate-cusped bubble coalescence (presented at [35]), and two cases of two-unequal bubble coalescences in this study. This demonstrates that the stage of liquid drainage is an accelerating process for all three bubble coalescences. This acceleration can be attributed to (i) the negative pressure at the leading bubble wake; (ii) the shear-thinning effect that causes a reduction of the apparent viscosity of the compressed liquid from the trailing bubble; (iii) the viscoelastic effect to recoil the circulated upward flow from the leading bubble to the rear of trailing bubble. These three factors generate a dragging force and a pushing force to accelerate the trailing bubble to come closer to the leading bubble. However, the case of two-equal oblate-cusped bubbles coalescing has less acceleration than the other cases of two-unequal bubbles coalescing. This is because a large bubble, no matter whether a leading bubble or a trailing bubble, can either generate a lower pressure that enhances the induction of the small trailing bubble or can reduce lower apparent viscosity to decrease the drag force opposite to itself. On the other hand, it is surprisingly to note that the two cases of two-unequal bubble coalescences have almost the same time lags of coalescing.

4. Concluding remarks

The course of the instantaneous flow structure, streamline and the shear stress contours for the in-line two-unequal bubble coalescences in a two-dimensional bubble column with a non-Newtonian fluid has been presented. The shear-thinning and viscoelasticity play important factors on the mechanisms of the two-unequal bubble coalescence in the non-Newtonian fluids. Along with the negative pressure at the leading bubble wake, a reducing viscosity by shear-thinning and a circulated upward flow from the leading bubble by viscoelasticity can, respectively, generate a dragging force and a pushing force to accelerate the trailing bubble to approach the leading bubble. The acceleration for two-unequal bubble coalescence is larger than that of two-equal bubble coalescence and no difference on the acceleration is observed if the large leading bubble and the small trailing bubble are switched. As the trailing bubble came closer to the leading bubble, the liquid between two bubbles was compressed, drained out, and circulated to the rear of the trailing bubble due to the viscoelastic effect. The

drainage flow combined with the circulated flow from the leading bubble recoiled back to the trailing bubble and caused it to have a serial deformation. At the same time, the leading bubble was also suppressed and deformed by the upward flow from the trailing bubble.

Acknowledgement

The work was supported by the National Science Council grant NSC-96-2214-E-194-035 in Republic of China.

References

[1] L.-S. Fan, Gas–Liquid–Solid Fluidization Engineering, Butterworths, Stoneham, MA, 1989.
[2] W.-D. Deckwer, Bubble Column Reactors, John Wiley and Sons, New York, 1992.
[3] R.P. Chhabra, D. DeKee, Fluid particles in rheologically complex media, in: Transport Processes in Bubbles, Drops and Particles, Hemisphere, New York, 1992.
[4] E. Zana, L.G. Leal, The dynamics and dissolution of gas bubbles in a viscoelastic fluid, Int. J. Multiphase Flow 4 (1978) 237.
[5] L.-S. Fan, K. Tsuchiya, Bubble Dynamics in Liquids and Liquid–Solid Suspension, Butterworth–Heinenann, Stoneham, MA, 1990.
[6] R.P. Chhabra, Bubbles, Drops, and Particles in Non-Newtonian Fluids, CRC Press Inc., Boca Raton, FL, 1992.
[7] F. Raymond, J.M. Rosant, A numerical and experimental study of the terminal velocity and shape of bubbles in viscous liquids, Chem. Eng. Sci. 55 (2000) 943–955.
[8] M. Martín, F.J. Montes, M.A. Galán, Bubble coalescence at sieve plates. II. Effect of coalescence on mass transfer. Superficial area versus bubble oscillations, Chem. Eng. Sci. 62 (2007) 1741–1752.
[9] J.R. Crabtree, J. Bridgwater, Bubble coalescence in viscous liquids, Chem. Eng. Sci. 26 (1971) 839.
[10] K. Akita, F. Yoshida, Bubble size, interfacial area and liquid-phase mass transfer coefficient in bubble columns, Ind. Eng. Chem. 12 (1974) 84–91.
[11] I. Komasawa, I. Otake, M. Kamojima, Wake behind and its effect on interaction between spherical-cap bubble, J. Chem. Jpn. 13 (1980) 103.
[12] M.J. Prince, H.W. Blanch, Bubble coalescence and break-up in air-sparged bubble columns, AIChE J. 36 (1990) 1485–1499.
[13] T. Miyahara, T. Hayashino, Size of bubbles generated from perforated plates in non-Newtonian liquids, J. Chem. Eng. Jpn. 28 (1995) 596–600.
[14] G. Marrucci, A theory of coalescence, Chem. Eng. Sci. 24 (1969) 975–985.
[15] E. Camarasa, C. Vial, S. Poncin, G. Wild, N. Midoux, J. Bouillard, Influence of coalescence behaviour of the liquid and of gas sparging on hydrodynamics and bubble characteristics in a bubble column, Chem. Eng. Proc. 38 (1999) 329–344.
[16] J. Zahradník, G. Kuncová, M. Fialová, The effect of surface active additives on bubble coalescence and gas holdup in viscous aerated batches, Chem. Eng. Sci. 54 (1999) 2401–2408.
[17] J. Grienberger, Untersuchung und Modellierung von Blasensaulen, Thesis, University of Erlangen–Nuremberg (1992).
[18] S. Narayanan, L.H.J. Goossens, N.W.F. Kossen, Coalescence of two bubbles rising in line at low Reynolds number, Chem. Eng. Sci. 29 (1974) 2071.
[19] N.H. Sagert, M.J. Quinn, The coalescence of gas bubbles in dilute aqueous solutions, Chem. Eng. Sci. 33 (1978) 1087.
[20] A.K. Chesters, G. Hofman, Bubble coalescence in pure liquids, Appl. Sci. Res. 38 (1982) 237.
[21] K.S. Shiloh, S. Sideman, W. Resnick, Coalescence and break-up in dilute polydispersions, Can. J. Chem. Eng. 51 (1973) 542.
[22] K. Tsuchiya, L.-S. Fan, Near-wake structure of a single gas bubble in a two-dimensional liquid–solid fluidized bed: vortex shedding and wake size variation, Chem. Eng. Sci. 43 (1988) 1167.
[23] N. DeNevers, J.-L. Wu, Bubble coalescence in viscous fluids, AIChE J. 17 (1971) 182.
[24] D. Bhaga, M.E. Weber, Bubbles in viscous liquids: shapes, wakes and velocities, J. Fluid Mech. 105 (1981) 61.
[25] W.F. Bessler, H. Littman, Experimental studies of wakes behind circularly capped bubbles, J. Fluid Mech. 185 (1987) 137.
[26] O. Hassager, Negative wake behind bubbles in non-Newtonian liquids, Nature 279 (1979) 402.
[27] C. Bisgaard, O. Hassager, An experimental investigation of velocity fields around spheres and bubbles moving in non-Newtonian liquid, Rheol. Acta 21 (1982) 537.
[28] D. Funfschilling, H.Z. Li, Flow of non-Newtonian fluids around bubbles: PIV measurements and birefringence visualization, Chem. Eng. Sci. 56 (2001) 1137.
[29] T.-J. Lin, G.-M. Lin, An experimental study on flow structures of a single bubble rising in a shear-thinning viscoelastic fluid with a new measurement technique, Int. J. Multiphase Flow 31 (2005) 239.
[30] A. Acharya, J. Ulbrecht, Note on the influence of viscoelasticity on the coalescence rate of bubbles and drops, AIChE J. 24 (1978) 348.
[31] D. Dekee, P.J. Carreau, J. Mordarski, Bubble velocity and coalescence in viscoelastic liquids, Chem. Eng. Sci. 41 (1986) 2273.
[32] D. Dekee, R.P. Chhabra, A photographic study of shapes of bubbles and coalescence in non-Newtonian polymer solutions, Rheol. Acta 27 (1988) 656.
[33] H.Z. Li, Y. Mouline, D. Funfschiling, P. Marchal, L. Choplin, N. Midoux, Evidence for in-line bubble interactions in non-Newtonian fluids, Chem. Eng. Sci. 53 (1998) 2219.
[34] H.Z. Li, X. Frank, D. Funfschilling, Y. Mouline, Towards the understanding of bubble interactions and coalescence in non-Newtonian fluids: a cognitive approach, Chem. Eng. Sci. 56 (2001) 6419.
[35] T.-J. Lin, G.-M. Lin, The mechanisms of bubble coalescence in a non-Newtonian fluid, Can. J. Chem. Eng. 81 (2003) 476.
[36] M. Martín, J.M. García, F.J. Montes, M.A. Galán, On the effect of sieve plate configuration on the coalescence of bubbles, Chem. Eng. Proc.: Process. Intensification 47 (2008) 1799–1809.
[37] G. Brindley, J.M. Davies, K. Walters, Elastico-viscous squeeze films, J. Non-Newtonian Fluid Mech. 1 (1976) 19.
[38] R.C. Chen, I.S. Chou, Wake structure of a single bubble rising in a two-dimensional column, Exp. Therm. Fluid Sci. 17 (1998) 165.